CRYSTAL GROWTH & DESIGN

Article

pubs.acs.org/crystal

Chiral and Racemic Tetramorphs of 2,6-Di-*t*-Butylditolylfuchsone

Naba K. Nath,[†] Sanjay Nilapwar,[‡] and Ashwini Nangia*[,†]

[†]School of Chemistry, University of Hyderabad, Central University PO, Prof. C. R. Rao Road, Gachibowli, Hyderabad 500 046, India

[‡]Biomolecular Analysis Core Facility, University of Manchester, Michael Smith Building, Manchester, M13 9PT, U.K.

Supporting Information

ABSTRACT: The title molecule 4-(α,α-ditolylmethylene)-2,6-di-*t*-butyl-1,4-benzoquinone (abbreviated as di-*t*-butylditolylfuchsone and numbered 2-*t*-Bu) serendipitously afforded four concomitant polymorphs during routine purification by column chromatography in the same solvent elution fraction. Polymorph I crystallized in chiral space group $P2_1$. Polymorphs II, III, and IV crystallized in centrosymmetric space groups $P2_1/n$, *Pbca*, and $C2/c$, respectively. The role of bulky *t*-Bu groups for crystallization in the chiral space group is discussed for 2,6-ditolyl and 2,6-diphenyl fuchsones. α,α-Diphenylmethylene-2,6-di-*t*-butyl-1,4-benzoquinone (di-*t*-butyldiphenylfuchsone, 1-*t*-Bu) crystallized in $P2_1$ (one polymorph) and $P2_1/c$ (two polymorphs) space groups. Unfavorable steric repulsions due to bulky *t*-Bu groups result in voids in the crystal structures of centrosymmetric polymorphs II and III. Phase transformation of racemic structure II to III and finally to chiral polymorph I was monitored by thermal microscopy and differential scanning calorimetry. X-ray diffraction confirmed the phase transformation to be a single-crystal-to-single-crystal event. The chiral polymorph I is the stable modification in the tetramorphic system. Several randomly picked single crystals of 2-*t*-Bu polymorph I had the same absolute chirality by circular dichroism spectroscopy. A new molecule capable of exhibiting conformational chirality via atropisomerism is identified.

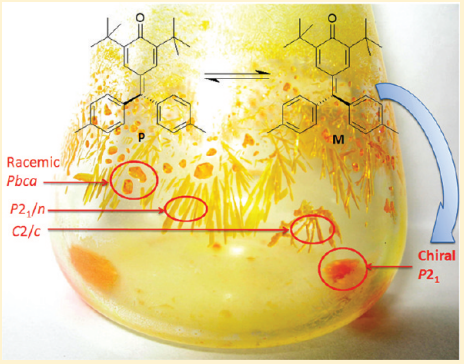

INTRODUCTION

Enantiopure optically active molecules must crystallize in one of the 65 Sohncke space groups. A racemic mixture of chiral molecules can crystallize as an achiral crystal or undergo spontaneous resolution to give two enantiopure crystals, the latter phenomenon being referred to as conglomerate crystallization or spontaneous resolution.[1,2] Crystallization as racemates is far more common, occurring in over 90% cases. Organic compounds that lack a stereogenic center or a plane of symmetry can adopt chiral conformations, leading to atropisomerism. The most classic example of chirality in molecules that lack a strereogenic center is ortho-disubstituted biphenyls, for example, 1,1′-bi-2-napthol. Such molecules can exist in a dynamic equilibrium of interconverting chiral conformations[3] in liquid state or in solution, but can freeze out as a single chiral conformation/configuration in the solid state to give chiral crystals. About 8−10% of achiral compounds in the Cambridge Structural Database crystallize in Sohncke space groups.[4] Such chiral crystals with non-centrosymmetric packing of molecules (i.e., those lacking an inversion center in the crystal structure) are important in materials applications such as electrooptic and nonlinear optical devices[5] and as catalysts for asymmetric synthesis.[6] The fundamental question of chiral crystallization is relevant to the origin of chirality in nature.[7]

Fuchsones can exist as rapidly interconverting chiral conformers in the liquid or solution state (Scheme 1). Fuchsones elicited early interest from crystallographers because of their photochromic properties and utility in dyes, photographic printing, etc. The methyl derivative of fuchsone, 1-Me, was the first compound in this family to exhibit polymorphism.[8] The crystallography of fuchsones lay dormant for several years until we revisited a few derivatives (series 1 and series 2, Scheme 2).[9] Surprisingly, a few fuchsones substituted with *t*-butyl and methyl R groups (1-*t*-Bu, 2-*t*-Bu, 1-Me) crystallized in chiral space groups, along with the more common racemic polymorphs. However, i-propyl derivatives crystallized in centrosymmetric space groups only. We report in this paper concomitant crystallization of four polymorphs of 2-*t*-Bu molecule during purification of the compound by column chromatography after synthesis. Both 1-*t*-Bu and 2-*t*-Bu showed

Scheme 1. Chiral Conformers of Fuchsones[a]

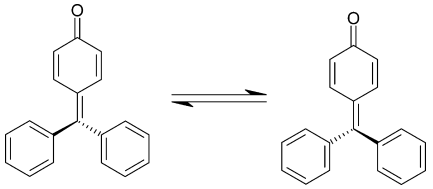

[a]The phenyl rings are oriented up or down with respect to the quinone ring plane in enantiomer conformations.

Received: December 14, 2011
Revised: January 19, 2012
Published: January 20, 2012

Scheme 2. Two Series of Fuchsones Studied[a]

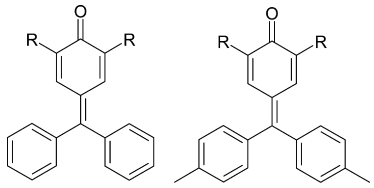

Series 1
R= Me, 1-Me
R= i-Propyl, 1-i-Pr
R= t-Bu, 1-t-Bu

Series 2
R= Me, 2-Me
R= i-Propyl, 2-i-Pr
R= t-Bu, 2-t-Bu

[a]Series 2 was obtained by replacing phenyl by *p*-tolyl groups.

preference toward chiral crystallization compared to other derivatives studied (Table 1).

Table 1. Space Groups of Fuchsone Polymorphs[a]

molecule	space group
1-Me[b,c]	$P2_1/c$, $\mathbf{P2_12_12_1}$, and $Pna2_1$
1-i-Pr[c]	*Pbca* and $P2_1/c$
1-*t*-Bu[c]	$P2_1/c$, $P2_1/c$, and $\mathbf{P2_1}$
2-Me[d]	$P2_1/c$, $P\bar{1}$, and $P2_1/c$
2-i-Pr[e]	$P2_1/n$
2-*t*-Bu[e]	$\mathbf{P2_1}$, $P2_1/n$, *Pbca*, $C2/c$

[a]Sohncke space groups are in bold. [b]Ref 8. [c]Ref 9a. [d]Ref 9b. [e]This paper.

RESULTS AND DISCUSSION

Series 1 fuchsones were reported in a previous publication.[9a] The crystallization, characterization and stability of chiral polymorph I ($P2_1$) and centrosymmetric structures II, III, and IV ($P2_1/n$, *Pbca*, $C2/c$; Table 2) of 2-*t*-Bu fuchsone are reported in this paper.

2,6-Di-*t*-Butylditolylfuchsone (2-t-Bu). 2-*t*-Bu was synthesized by the acid-catalyzed arylation of 2,6-di-*t*-butylphenol with 4,4′-dimethylbenzyhydrol (Scheme 3). The product ketone after MnO_2 oxidation was subjected to silica gel chromatography for purification in the usual way. We serendipitously observed that eluting the column with 2−3% EtOAc + *n*-hexane solvent deposited crystals along the side walls in one of the erlenmeyer (conical) flask fractions (Figure 1). Crystals of four different morphologies could be identified in the same crystallization vessel: thin plate (form II), thin needle/fiber (form IV), thick plate (form III), and large blocks (form I). Careful handling of these single crystals with a needle and mounting on the X-ray diffractometer confirmed that they are polymorphs. They are named as polymorphs I, II, III, and IV of 2-*t*-Bu according to the order in which they were characterized by single crystal X-ray diffraction, which is the best quality crystal first and the not so good ones later on. Polymorph I crystallized in chiral space group $P2_1$, whereas polymorphs II, III, and IV crystallized in centrosymmetric arrangement in $P2_1/n$, *Pbca*, and $C2/c$ space group (Table 2). Even though the block morphology crystals of form I were stuck to each other in a lump (see bottom of flask in Figure 1), they could be easily separated with a needle and produced good quality crystal data. The asymmetric unit of structures I−III contained one molecule each, whereas polymorph IV has a half molecule residing on the 2-fold axis. Crystallization of 2-*t*-Bu from various solvents in a routine crystallization afforded only polymorph I. The conditions for the concomitant crystallization[10] of 2-*t*-Bu polymorphs are detailed in the Experimental Section.

Conformational Chirality of 2-*t*-Bu Molecule. Fuchsones can adopt chiral conformations. The molecule is achiral (meso) in the perfectly flat conformation, but in reality the two phenyl rings are twisted to relieve steric crowding of H-atoms and this can give enantiomeric conformations (Figure 2a,b). The enantiomer conformations are rapidly interconverting in the liquid or solution state. It is possible to freeze out one or both enantiomers in the solid state leading to conglomerate crystallization or racemic crystals, respectively. The conformational chirality of 2-*t*-Bu molecule arises due to the spatial arrangement of the *p*-tolyl groups making them non-superimposable mirror image conformations.

In order to know the sense of chirality in fuchsones, these molecules were compared to the axial chirality in ortho-biphenyls, allenes, and helicenes. Among them helicenes appeared to be closest to define chirality in fuchsones.[11] If the benzoquinone ring is considered as lying in a plane with the carbonyl group pointing away from the viewer, the *p*-tolyl groups reside on either side (up and down, Figure 2c). Now a helical movement about the benzoquinone plane, from up to down via the carbon atoms (highlighted as circles in Figure 2d) in the order: methyl C (up tolyl) → phenyl C (up tolyl) → methylene C (in plane) → phenyl C (down tolyl) → methyl C (down tolyl), is either clockwise (right-handed) or anticlockwise (left-handed). Therefore, similar to helicenes, chirality in fuchsones can be defined as P (plus) for clockwise movement and M (minus) for anticlockwise movement (Figure 2d).

Crystal Structure Analysis. A single enantiomer of 2-*t*-Bu is present in the crystal structure of polymorph I. Helices are formed via C−H···O hydrogen bonds (C29−H29C···O1, 2.41 Å, 154.8°) around a 2-fold screw axis (Figure 3a). In contrast, helices of opposite handedness (shaded blue and red for right- and left-handed) are present in crystal structures II−IV (Figure 3b−d). Crystallographic data and hydrogen bond parameters are summarized in Tables 2 and 3.

In the crystal structure of polymorph I, the oxygen acceptor is involved in bifurcated C−H···O hydrogen bonds (C29−H29C···O1, 2.41 Å, 154.8° and C28−H29C···O1, 2.56 Å, 176.8°) to connect neighboring parallel helices. The helical chains are stacked and connected via a C−H···π interaction (2.56 Å, 163.2°) to complete the chiral molecular packing (Figure 4). The molecular chirality of 2-*t*-Bu in polymorph I is M or (−) or left-handed (as discussed in the next section).

Helical motifs are also present in polymorphs II−IV except that these crystal structures are centrosymmetric and contain helices of opposite handedness in the unit cell. C−H···O hydrogen bonded (C16−H16···O1, 2.22 Å, 158.4°) helices are connected via C−H···π interactions (C13−H13···π, 2.65 Å, 147.0°; C19−H19···π, 2.77 Å, 124.6° and C9−H9···π, 2.70 Å, 167.1°) between inversion-related molecules to form an empty channel in the crystal structure of polymorph II (Figure 5). The channel diameter is too small (<4.8 Å) for any solvent inclusion.

The view of a single helix in polymorph III (Figure 6a) is similar to II (Figure 5a) with the minor difference that the inversion related helix is stacked with offset, thereby capping the void on both sides (Figure 6b).

The molecule in crystal structure IV resides on a 2-fold axis in $C2/c$ space group. There is no C−H···O interaction up to the normal distance cutoff of 2.8 Å (a long C16−H16A···O1

dx.doi.org/10.1021/cg201652h | *Cryst. Growth Des.* 2012, 12, 1613−1625

Table 2. Crystallographic Data and Cell Refinement Parameter

compound	2-*t*-Bu form I	2-*t*-Bu form II	2-*t*-Bu form III	2-*t*-Bu form IV
chemical formula	$C_{29}H_{34}O$	$C_{29}H_{34}O$	$C_{29}H_{34}O$	$C_{29}H_{34}O$
formula weight	398.56	398.56	398.56	398.56
crystal system	monoclinic	monoclinic	orthorhombic	monoclinic
space group	$P2_1$	$P2_1/n$	$Pbca$	$C2/c$
T/K	100	100	100	100
a/Å	6.0525(8)	9.0435(8)	15.8153(14)	12.5468(14)
b/Å	19.535(3)	16.2029(15)	17.4890(15)	23.813(3)
c/Å	10.3567(14)	17.1008(16)	17.9924(16)	9.2568(10)
α/°	90	90	90	90
β/°	103.489(2)	95.993(2)	90	121.033(2)
γ/°	90	90	90	90
Z	2	4	8	4
V/Å^3	1190.7(3)	2492.1(4)	4976.6(8)	2369.8(4)
D_{calc}/g cm^{-3}	1.112	1.062	1.064	1.117
μ/mm^{-1}	0.065	0.062	0.062	0.065
reflns collected	12340	23016	45143	11335
unique reflns	4703	4358	4412	2104
observed reflns	4580	3719	3767	1708
R_1 [$I > 2\sigma(I)$]	0.0322	0.0586	0.0509	0.0550
wR_2 [all]	0.0812	0.1176	0.1169	0.1137
goodness-of-fit	1.060	1.146	1.116	1.063
diffraction density max/min	0.224/−0.173	0.227/−0.279	0.289/−0.181	0.255/−0.191
diffractometer	SMART APEX CCD	SMART APEX CCD	SMART APEX CCD	SMART APEX CCD

2-i-Pr	2-Me form I	2-Me form II	2-Me form III
$C_{27}H_{30}O$	$C_{23}H_{22}O$	$C_{23}H_{22}O$	$C_{23}H_{22}O$
370.51	314.41	314.41	314.41
monoclinic	monoclinic	triclinic	monoclinic
$P2_1/n$	$P2_1/c$	$P\bar{1}$	$P2_1/c$
100	100	100	100
8.5454(9)	7.6297(5)	7.4822(6)	12.869(3)
15.2329(16)	12.5889(8)	8.1328(6)	17.255(4)
17.3166(18)	18.2064(11)	15.3014(11)	7.960(2)
90	90	97.5620(10)	90
98.015(2)	95.4670(10)	101.0460(10)	99.436(5)
90	90	102.9920(10)	90
4	4	2	4
2232.1(4)	1740.76(19)	875.49(11)	1743.6(7)
1.103	1.200	1.193	1.198
0.065	0.071	0.071	0.071
20509	17000	9080	16414
3798	3233	3406	3085
3284	3089	3235	2472
0.0547	0.0498	0.0430	0.0755
0.1324	0.1300	0.1107	0.1665
SMART APEX CCD	SMART APEX CCD	SMART APEX CCD	SMART APEX CCD

Scheme 3. Synthetic Route to 2-*t*-Bu Fuchsone[a]

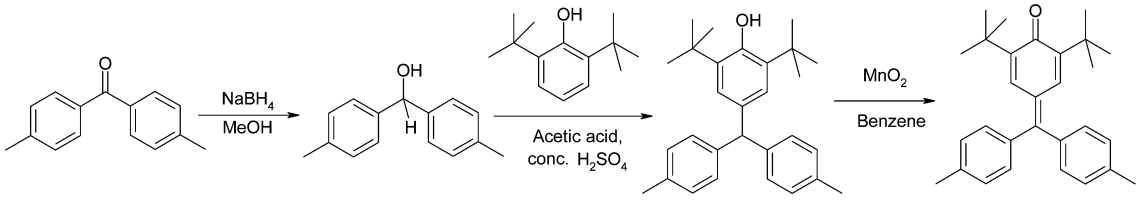

[a]Other derivatives were synthesized analogously.

of 2.98 Å, 137.0°) and a C−H···π interaction (C11−H11···π 2.76 Å, 176.6°) connects molecules in adjacent stacks (Figure 7).

A slight similarity may be noted between substructures of forms II and IV by viewing their packing down the *a*-axis and *c*-axis, respectively. C−H···π interactions connecting the

dx.doi.org/10.1021/cg201652h | *Cryst. Growth Des.* 2012, 12, 1613−1625

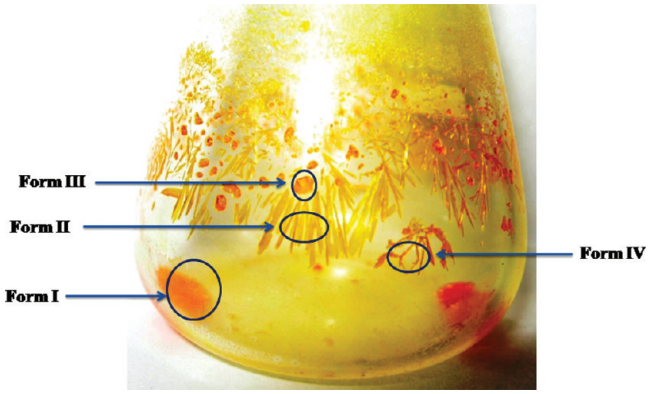

Figure 1. A crystallization batch to show four 2-*t*-Bu concomitant polymorphs deposited on the walls of an erlenmeyer flask fraction eluted using 2% EtOAc−*n*-hexane.

molecular columns are identical in form II and IV, but they differ in the way molecules are arranged: the carbonyl groups of molecules line up parallel in form IV, whereas adjacent columns of form II are aligned at 90°. Despite these similarities in local domains, the gross differences between these structures qualify them to be called polymorphs.

Other Crystals Structures in This Series. 2-i-Pr forms bifurcated C−H···O hydrogen bonds (C10−H10···O1, 2.29 Å, 152.1° and C27−H27C···O1, 2.56 Å, 140.9°) with two inversion related molecules which are connected via C−H···π interaction (C13−H13···π, 2.73 Å, 141.9°) (Figure 8). No new polymorphs were found for this compound during our crystallization trials.

Conformation of 2-*t*-Bu in Crystal Structures. The conformation of polymorph I (red, Figure 9, torsion angles are listed in Table 4) is quite different from those of other three polymorphs. Several of phenyl torsion angles are in range 42−47°, with extreme values of 35° and 63° in conformational polymorphs[12] of 2-*t*-Bu.

To summarize the main structural trends in fuchsones, 1-Me gave three polymorphs of which one is chiral, 1-i-Pr is dimorphic (both racemic), 1-*t*-Bu is trimorphic (one chiral), and 2-Me is trimorphic (all racemic) (listed in Table 1). The main objective in the present study was to find out if there is any steric effect of the R group (= *t*-Bu) flanking the quinone ring to result in chiral polymorphs?

Resolution of 2-*t*-Bu Enantiomers. To find out if the sense of chirality in the $P2_1$ single crystals of 2-*t*-Bu is the same or opposite of randomly picked crystals, the absolute configuration was determined by recording reflections using Cu−Kα radiation. Three good quality single crystals of 2-*t*-Bu were selected from the same column chromatography fraction flask (now with 20% EtOAc + *n*-hexane solution because the more polar solvent gave superior quality single crystals of the chiral variety for absolute configuration) and mounted on the X-ray diffractometer. The Flack parameter[13] for different single crystal X-ray structures of form I gave a value of 0.0(2) in each case (Cu−Kα crystallographic data are listed in Table S1). In the absence of a heavy atom scatter, such as halogen or sulfur (atomic number >10), the difference between the Friedel pairs reflections was small, and so the standard uncertainty of the Flack parameter is high. A consistent value of 0 suggested that the three crystal structures of 2-*t*-Bu had the M (minus) absolute configuration (Figure S1). Circular dichroism (CD) spectroscopy is useful to establish the absolute configuration of

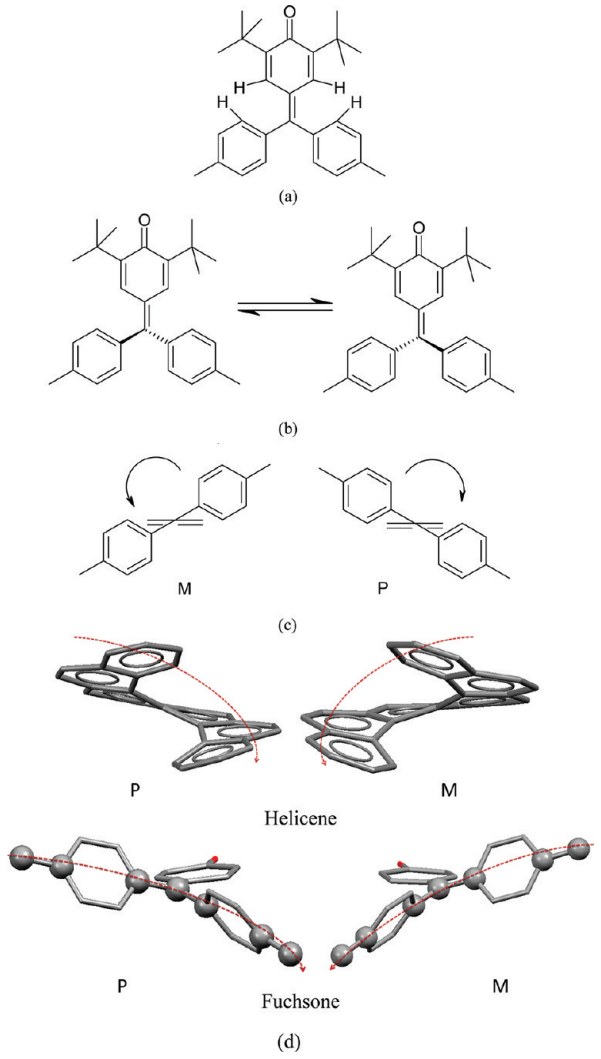

Figure 2. (a) The flat conformation of 2-*t*-Bu suffers from severe H···H repulsion. (b) The molecule hence exists (b) as a dynamic equilibrium of two enantiomers in solution or melt. (c) The enantiomers are named as P (plus) and M (minus) considering the benzoquinone ring as lying in a plane and the *p*-tolyl groups residing on either side. (d) The sense of chirality in fuchsone is compared to the well-known helicene.

a chiral crystalline solid,[14] and it can also provide information about enantiomer interconversion in solution or liquid state. Solid-state CD spectra (Figure 10) recorded on the bulk sample from four different crystallization batches (*n*-hexane, $CHCl_3$, 10% EtOAc + *n*-hexane, and CH_3CN solution) showed the presence of a single enantiomer of 2-*t*-Bu with the same absolute chirality. The variation in intensity of CD signal curve (e.g., green to black line) in the solid state is batch-to-batch variation. Interestingly, the opposite enantiomer was not indicated in any of the CD spectra recorded. Such an enantiomer selection or conglomerate crystallization is known in compounds exhibiting conformational chirality.[15] CD spectra of the chiral crystal recorded in ethanol solution at 1 min time interval did not show any noticeable signal (Figure 11), suggesting that the rate of racemization is very fast in solution on the time scale of conventional CD spectroscopy.

Why *t*-Butyl Group for Chiral Crystallization? A conformationally flexible molecule lacking a chiral center or an axis of symmetry can crystallize in chiral space groups when

dx.doi.org/10.1021/cg201652h | *Cryst. Growth Des.* 2012, 12, 1613−1625

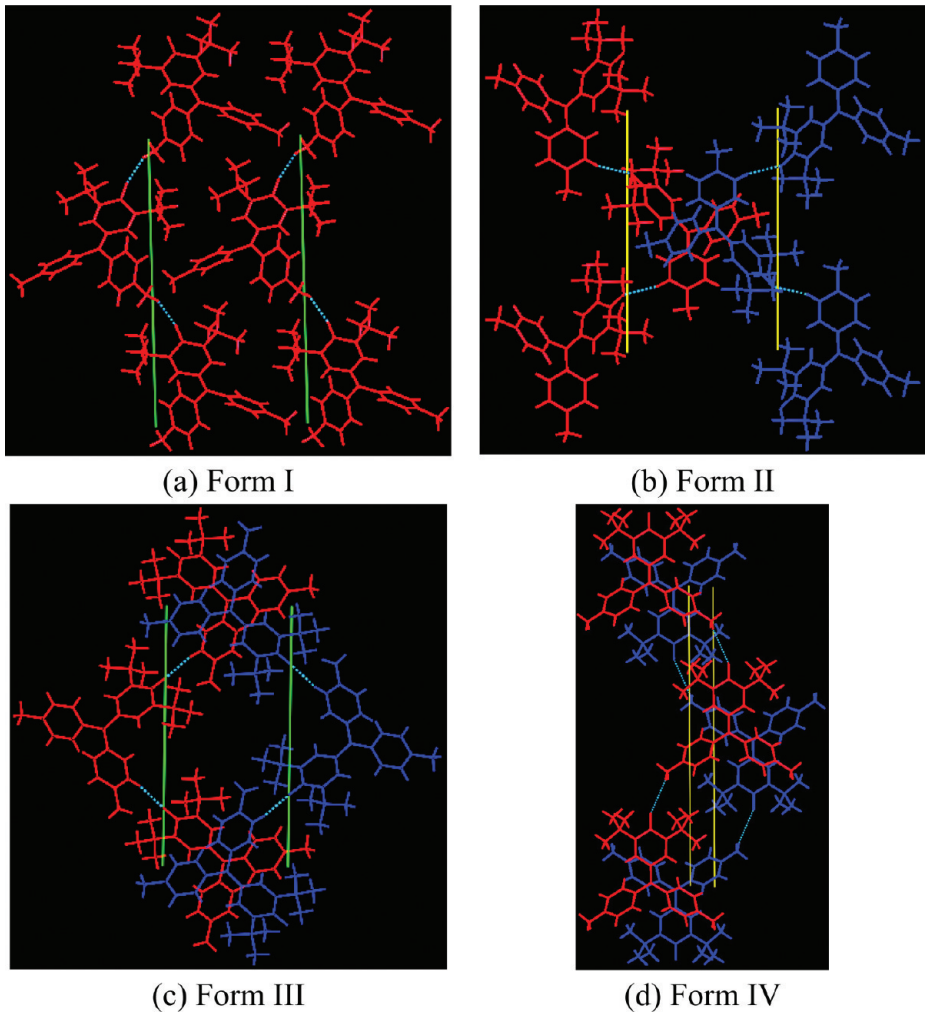

Figure 3. 2-*t*-Bu polymorph: (a) form I contains a helix of single handedness, whereas forms II–IV (b, c, d) contain helices of opposite handedness (shown in different colors, blue and red for right- and left-handed helices).

Table 3. Hydrogen Bond Parameters in 2-*t*-Bu Polymorphs

interaction	H···A/Å	D···A/Å	∠D–H···A/°	symmetry code
		Form I		
C(29)–H(29C)···O(1)	2.41	3.421(2)	154.8	$1 - x, -1/2 + y, 2 - z$
C(28)–H(29C)···O(1)	2.56	3.643(2)	176.0	$1 - x, 1/2 + y, 1 - z$
C(21)–H(21A)···O(1)	2.33	3.027(2)	120.3	intramolecular
C(22)–H(22B)···O(1)	2.26	2.959(2)	120.5	intramolecular
C(25)–H(25C)···O(1)	2.32	3.010(2)	119.8	intramolecular
C(26)–H(26A)···O(1)	2.32	3.009(2)	119.5	intramolecular
		Form II		
C(16)–H(16) ···O(1)	2.22	3.249(2)	158.4	$1/2 - x, -1/2 + y, 3/2 - z$
C(21)–H(21C)···O(1)	2.33	3.014(2)	119.6	intramolecular
C(22)–H(22A) ···O(1)	2.31	2.985(2)	119.1	intramolecular
C(25)–H(25B)···O(1)	2.36	3.036(2)	119.3	intramolecular
C(26)–H(26B)···O(1)	2.27	2.964(2)	120.2	intramolecular
		Form III		
C(16)–H(16)···O(1)	2.18	3.242(2)	166.5	$-x, -1/2 + y, 1/2 - z$
C(21)–H(21B)···O(1)	2.34	3.018(2)	119.4	intramolecular
C(22)–H(22B)···O(1)	2.29	2.984(2)	120.4	intramolecular
C(25)–H(25A)···O(1)	2.31	2.990(2)	119.4	intramolecular
C(26)–H(26C)···O(1)	2.30	2.991(2)	119.9	intramolecular
		Form IV		
C(16)–H(16)···O(1)	2.98	3.847(2)	137.0	$1/2 - x, -1/2 + y, 1/2 - z$

dx.doi.org/10.1021/cg201652h | *Cryst. Growth Des.* 2012, 12, 1613–1625

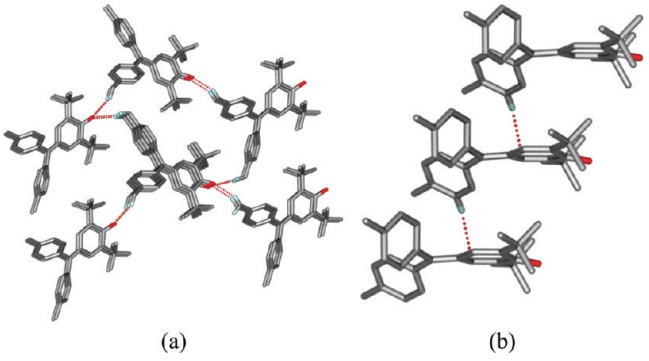

Figure 4. (a) Bifurcated C−H···O hydrogen bonds connect helices in the crystal structure of polymorph I, and (b) C−H···π interaction between the stacked quinone planes. Nonbonded H-atoms are removed for clarity.

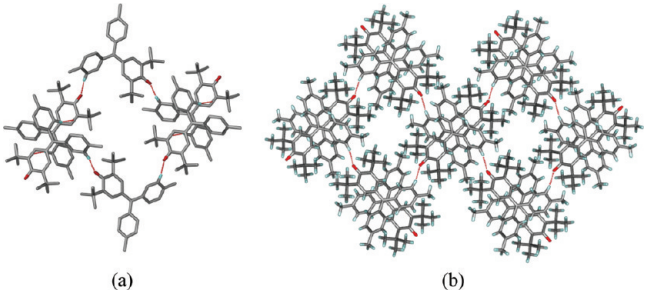

Figure 5. In form II, two antiparallel C−H···O hydrogen bonded helices are connected by C−H···π interactions between inversion related molecules (a). Bulky *t*-butyl groups loosely close pack to form a small cavity (b). Nonbonded H-atoms are removed for clarity.

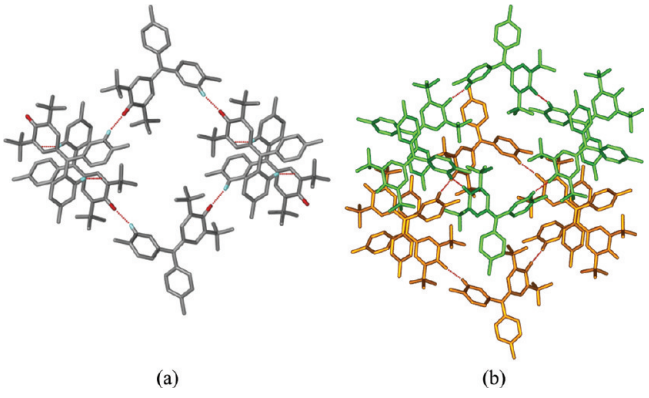

Figure 6. In form III, two opposite C−H···O hydrogen bonded helices are connected by C−H···π interaction between inversion related molecules forming cavity (a). Another pair of opposite handed helices covers the cavity (shown in different colors) (b). Nonbonded H-atoms are removed for clarity.

the energy barrier for interconversion is high due to steric factors (e.g., ortho-biphenyls). If the molecule is conformationally locked and cannot convert to its mirror image under the given conditions, the compound can exhibit configuration chirality. The conformation energy map for a model compound of 2-*t*-Bu, in which the six-member quinone ring was truncated to reduce excessive computation time, was calculated at 10° torsion angle intervals for rotation of the Me groups in the *t*-Bu fragment (Figure 12). The abrupt drop in energy between the 140 and 150° torsion angle is due to relief of Me···O═C strain as the methyl group rotates to reach a 150° angle (see Figure S2,

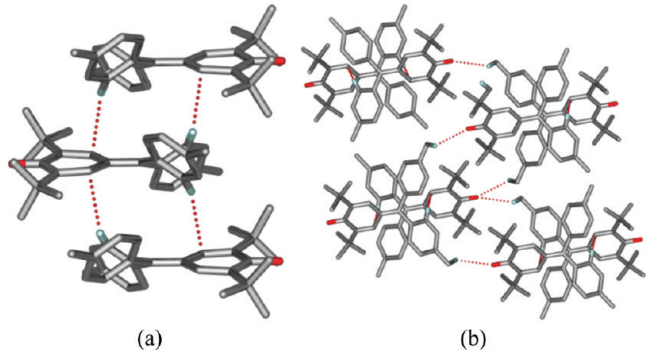

Figure 7. (a) C−H···π dimers of polymorph IV are connected (b) by a long C−H···O interaction (b). Nonbonded H-atoms are removed for clarity.

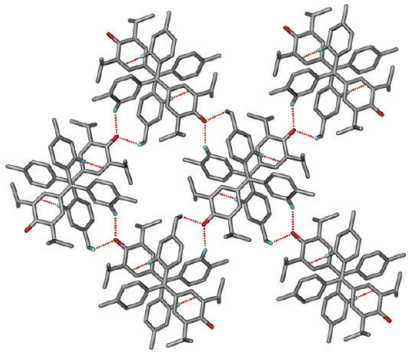

Figure 8. Bifurcated C−H···O hydrogen bonds connect inversion related molecules in 2-i-Pr, which are in turn connected via C−H···π interaction to make stacks.

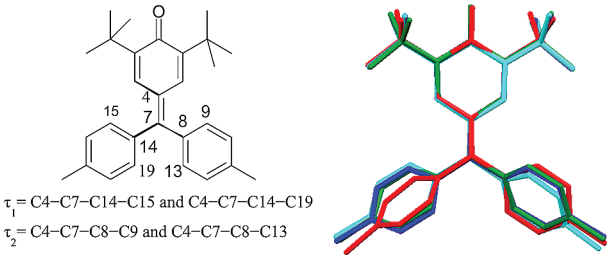

Figure 9. Overlay diagram to show the four conformers: form I (red), form II (blue), form III (cyan), and form IV (green). The M enantiomer is used in the molecular overlay.

Table 4. Torsion Angles of 2-*t*-Bu Conformers in the Crystalline State

polymorph	torsion angles (deg)
Form I	C4−C7−C14−C15 = 38.6(2) and C4−C7−C8−C9 = 63.2(2)
Form II	C4−C7−C14−C15 = 35.6(3) and C4−C7−C8−C9 = 47.0(3)
Form III	C4−C7−C14−C15 = 42.3(2) and C4−C7−C8−C9 = 47.2(2)
Form IV	C4−C5−C6−C7 = 42.8(2)

Supporting Information). An energy barrier of 5 kcal/mol between the energy minima is sufficiently high at room temperature (the temperature at which crystals begin to appear, RT = 0.6 kcal/mol at 300 K); it is able to arrest facile interconversion between *t*-Bu conformers (enantiomers). The frozen chiral conformation will lead to crystallization of a single enantiomer in the solid- state. There is no simple explanation for why all the chiral crystal batches of 2-*t*-Bu that we examined exhibited

dx.doi.org/10.1021/cg201652h | *Cryst. Growth Des.* 2012, 12, 1613−1625

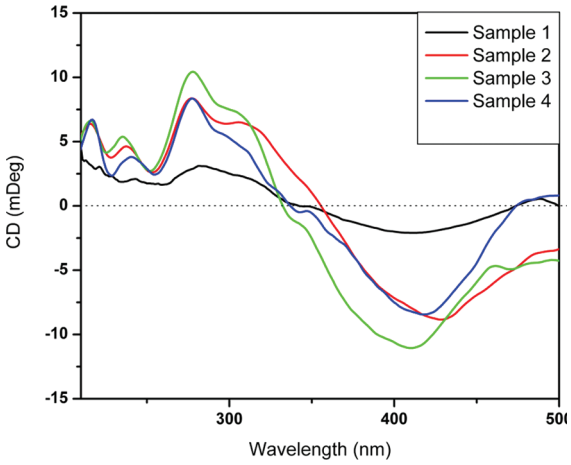

Figure 10. Solid-state CD spectra of four different batches of crystallization show optical activity for the same enantiomer conformation of 2-t-Bu. Sample 1 = form I obtained from *n*-hexane, Sample 2 = form I obtained from $CHCl_3$, Sample 3 = form I obtained from EtOAc + *n*-hexane (10:90 mixture), Sample 4 = form I obtained from CH_3CN.

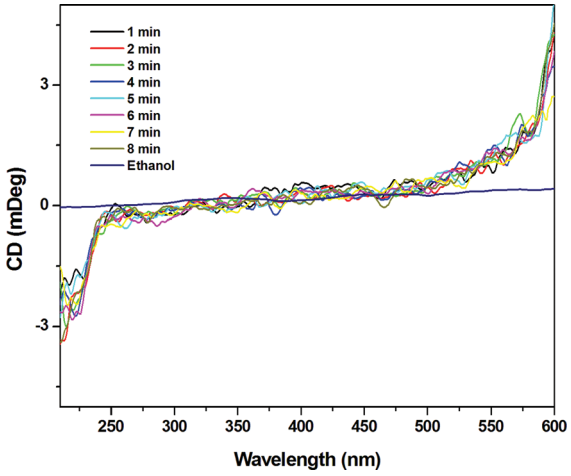

Figure 11. Solution-state CD spectra recorded for form I crystals of 2-*t*-Bu in ethanol solution recorded at 1 min intervals up to 8 min. There is no noticeable CD signal indicating very fast racemization in solution.

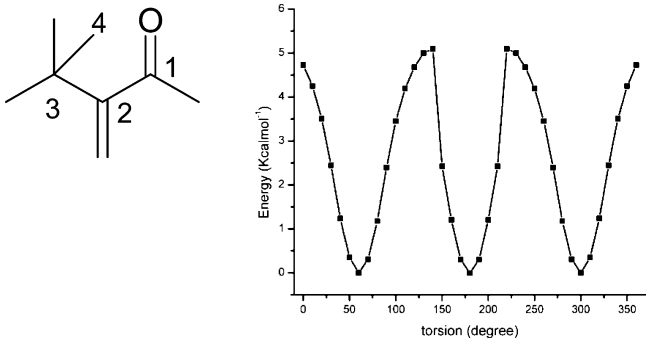

Figure 12. Conformer energy plot for a model molecule calculated at 10° torsion angle rotation of Me carbon of the *t*-Bu group between τ_1 = 0−180°. The energy profile is symmetric about τ_1 = 180°. Conformer energies were calculated in Gaussian 03 (B3LYP/6-31G (d,p)).

M helicity. However, once an M batch of crystals of 2-*t*-Bu crystals were produced, subsequent batches could well have been driven to M chirality by seeding. We have no proper explanation for nonstochastic homochiral M crystallization from the experiments carried out so far.

The arguments for preferential chiral crystallization presented in this paper will apply to 1-*t*-Bu fuchsone (Ph instead of *p*-Tol) reported recently by us.[9a] The first compound of this series, 1-Me, crystallized as chiral $P2_12_12_1$ polymorph and racemic $P2_1/c$ and $Pna2_1$ crystal structures.[8,9] The calculated energy barrier for CH_3 rotation is 1.4 kcal/mol.

The focus in this study was to understand the role of the bulky *t*-butyl group in promoting chiral crystallization, largely driven by the experimental observation that *t*-Bu fuchsones gave crystallization in Sohncke space groups. A totally different and somewhat more complex pathway for chiral crystallization could be via Ph group rotation at τ_1 and τ_2 (Figure 9). However, in this mechanism all fuchsones should have exhibited preferential chiral crystallization, which is not consistent with the experiments, and hence this possibility was not examined in the limited computational study.

Pidcock[4a] categorized achiral molecules which crystallized in chiral space groups into four groups: (1) rigid molecules with rotational point group symmetry, (2) rigid molecules with inversion or mirror point group symmetry, (3) conformationally flexible molecules possessing a high steric energy barrier for the conversion of the structure to the mirror image, and (4) conformationally flexible molecules with low steric energy barriers for interconverting to its mirror image. The *t*-butyl-fuchsones in this work fall in category (3), and a similar example (see Figure S3, Supporting Information) was pointed out in the database survey.[4a]

Conformationally locked achiral molecules are 6 times more likely to crystallize in a racemic space group compared to a Sohncke space group. A survey of the CSD (version 5.32, Nov 2011 update)[16] for achiral/racemic molecules containing the *t*-butyl group showed that crystallization in Sohncke space groups occurs in about 7.5% cases for polymorph sets for which both chiral and centrosymmetric crystal structure are reported. A detailed correlation of molecular structure and solid-state chirality for these CSD structures (refcodes listed in Table S2) is currently ongoing.

Phase Transformations. The stability of 2-*t*-Bu polymorphs was studied by hot stage microscopy, differential scanning calorimetry (DSC) and X-ray diffraction (XRD). Form II converted to form III and finally to form I, whereas form III converted directly to form I upon heating. Form IV is stable to heating.

Hot-stage microscopy (HSM) images of form II (Figure 13a) showed a crystal-to-crystal phase transition at 130 °C which continued up to 140 °C. A second crystal-to-crystal phase transition was observed at 160 °C which continued up to 176 °C, and ultimately melting was observed at 189 °C.

In order to confirm the phase changes visualized on HSM, a few crystals of form II (identified easily by their distinct thin plate morphology and by unit cell check, Figure S4) were heated to 130 °C in a temperature-controlled convection oven. Crystals were taken out after 6 h, cooled to room temperature, and their unit cell parameters were determined. They matched with 2-*t*-Bu form III. Again the same batch of crystals was heated to 165 °C for 6 h, and unit cell check confirmed that they have now converted to form I. Form III crystals underwent crystal to crystal phase transition at 146 °C and melted at 189 °C (Figure 13b). Therefore, the sequential phase changes upon heating are form II → form III and form III → form I. Form III

dx.doi.org/10.1021/cg201652h | *Cryst. Growth Des.* 2012, 12, 1613−1625

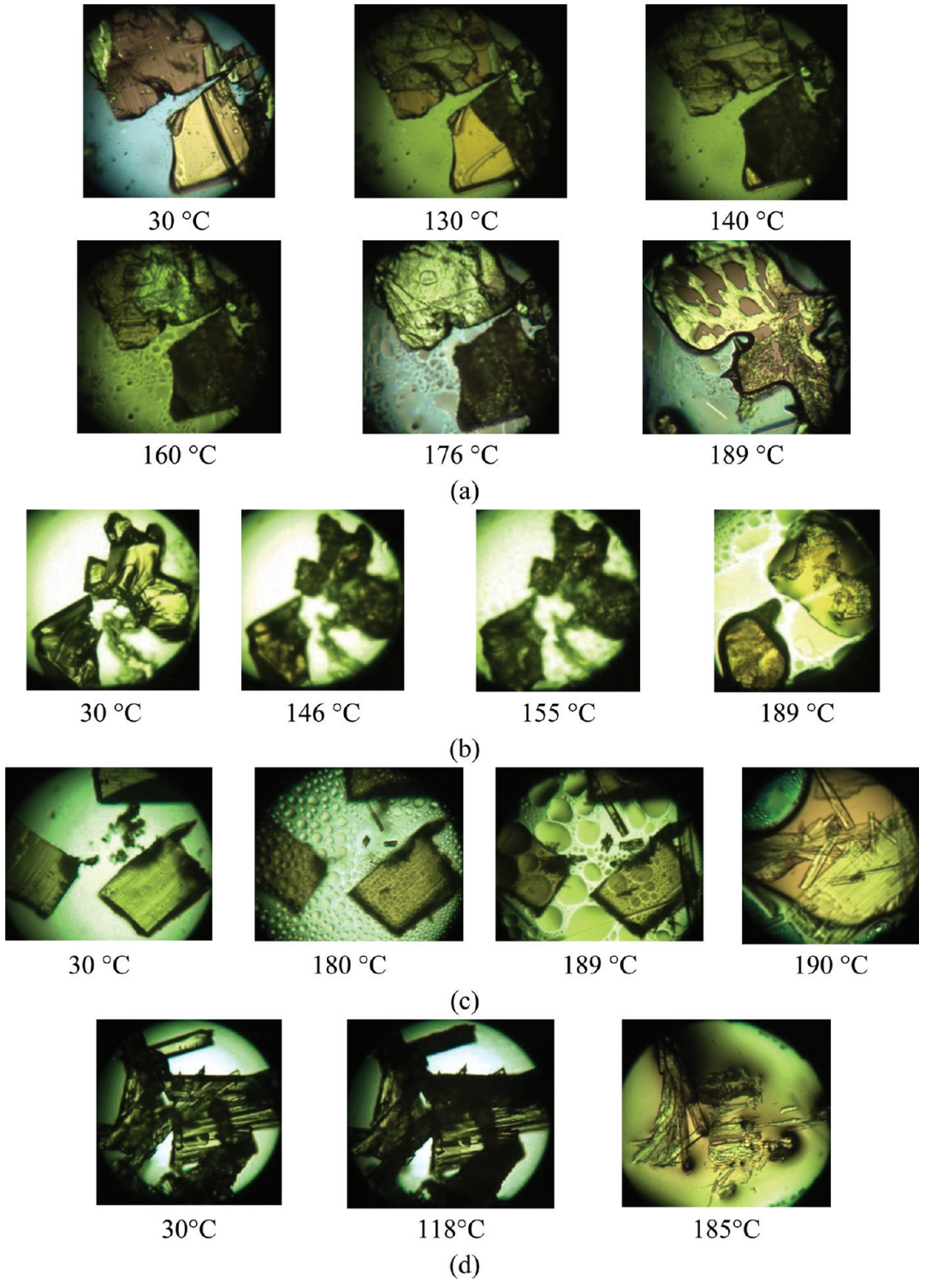

Figure 13. Hot stage microscopy images. (a) Two successive phase transitions in form II crystal at 130 °C (to form III) and 160 °C (to form I) and finally melting at 189 °C. (b) Form III transformed to form I at 146 °C and then melting occurred at 189 °C. (c) Form I indicated appearance of a new crystal near the melting point (180 °C) when the sample sublimed, but no phase change was noted. (d) Needle morphology crystals of Form IV melted at 185 °C.

crystals transformed to form I when kept at 160 °C for 6 h (Figure S5), thereby confirming the HSM observations. Heating form I crystals on HSM indicated a transformation at 180 °C due to sublimation. A unit cell check showed that the sublimed material after solidification was form I; there was no phase change (Figure 13c). Form IV crystals exhibited no phase change upon heating (Figure 13d). Even though single crystals of form II and III broke to small pieces upon heating, they still retained their crystalline nature and X-ray reflections could be recorded for unit cell comparison.

Single-crystal-to-single-crystal (SCSC) phase transition is as such uncommon, and only a few examples are reported for

dx.doi.org/10.1021/cg201652h | *Cryst. Growth Des.* 2012, 12, 1613–1625

organic, inorganic, and metal−organic systems.[17] The reason for such a rare occurrence of this phenomena is that single crystals often lose their mosaicity upon phase transition due to cooperative movement of atoms or molecules in the solid state. The mechanism behind SCSC transition of 2-*t*-Bu polymorph from racemic to chiral single crystal is under investigation.

No phase transition was observed for form I in DSC thermogram. In case of form II, there are two weak endotherms at about 155 and 172 °C, which correspond to the phase transitions that were observed in HSM and single crystal XRD experiments. The first endotherm corresponds to form II → III change and the second endotherm to form III → I change. DSC of form III showed a weak endotherm at about 160 °C for form III → I transformation, as was evident from HSM experiments. DSC thermograms of form I, form II, and form III are displayed in Figure 14. All these observations suggest that polymorphs II and III are enantiotropically related to form I, and that form I is the thermodynamic, stable polymorph. DSC of form IV crystals could not be measured because of very few single crystals in the concomitant batch.

Stability of Polymorphs. Ostwald[18] stated over a century ago that a system moves to thermodynamic equilibrium from an initial high energy state through minimal changes in free energy. Therefore, the polymorph that crystallizes first is the one which possesses the lowest energy barrier (highest energy, metastable). This form would then transform to the next lower energy polymorph until a thermodynamically stable state is reached, the so-called Ostwald's Law of Stages. It was observed during crystallization of the four polymorphs that forms II, III, and IV crystallized first on the walls of the flask and only after complete evaporation of the solvent were form I crystals observed. Therefore according to Ostwald's law of stages form I is the thermodynamically stable polymorph and forms II, III, and IV are kinetically metastable. The packing fraction and density of four polymorphs are listed in Table 5. Forms I and IV have almost similar packing fraction and density, and their values are greater than that for forms II and III. Crystal structures with higher density and packing fraction are usually more stable.

According to Wallach's rule,[19] again over a century old, racemic crystals are more stable than their chiral counterparts. Brook and Dunitz[20] carried out a systematic CSD survey in 1991 to validate Wallach's rule in a statistically significant set of crystal structures. They noted that for chiral compounds (resolvable enantiomers), racemic crystals have a greater average density compared to their enantiomers (by ca. 1% for 65 compounds analyzed). For achiral compounds to give chiral crystals (enantiomers interconvert rapidly in solution), the difference in density of chiral to racemic crystal was negligible (for 64 compounds analyzed). The quantity $\Delta(\%) = 100\,[(V/Z)_A - (V/Z)_R]/\{0.5[(V/Z)_A + (V/Z)_R]\}$, where A and R refer to chiral and racemic crystals and V/Z is the molecular volume, should be significantly positive for Wallach's rule to hold. For chiral compounds with resolvable enantiomers, the value of Δ is significantly positive, +0.92(29)%. Δ was found to be +0.20(34)% for 64 pairs of rapidly interconverting enantiomer compounds. On an average, the difference in density is not significantly different from zero, although in a few cases very high positive values of Δ were noted (e.g., +8.29% and +7.62%). In general, there were examples on both sides of Wallach's rule in the CSD study.[20]

In the case of 2-*t*-Bu the chiral crystal structure has a higher density and is more stable than racemic/centrosymmetric polymorphs, providing an exception to Wallach's rule. For the polymorph pairs I and II, I and III, and I and IV the value of Δ calculated using the above equation is −4.54%, −4.39%, and +0.49% giving inverse Wallach's rule for the first and second pair of 2-*t*-Bu fuchsone polymorphs.

We rationalize why the chiral crystal structure of 2-*t*-Bu form I has a higher density and is the most stable polymorph. The molecular packing in form I is mediated via C−H···O hydrogen bond (C29−H29C···O1 and C28−H28A···O1) from *p*-methyl groups of tolyl ring to carbonyl O in a bifurcated motif. The ortho H of tolyl ring is the donor in form II and form III for C16−H16···O1 interaction. Because the bulky *t*-butyl groups are placed very close to each other structures II and III (Figure 15), the molecular packing opens up to relieve *t*-Bu···*t*-Bu repulsion (bump−bump contact), and this results in lower density and packing fraction for polymorphs II and III (Table 5). The weak C16−H16A···O1 in form IV involves *p*-methyl C−H donor, similar to form I. The sterically bulky *t*-Bu groups therefore play a dual role. They promote preferential crystallization of the chiral polymorph by increasing the barrier to conformer interconversion and by destabilizing racemic crystal structures II and III.

CSD Search on Tetramorphs or More Numbers of Polymorphs. A CSD search (CCDC version 5.32, August 2010 update, 2011 update)[16] using the search terms polymorph, form, phase, or modification with 3D coordinate determined resulted in 14 460 hits. There are 27 tetramorphic, 10 pentamorphic, 2 hexamorphic, and 1 heptamorphic systems with crystallographic coordinates reported to date. There are only two tetramorphic systems for which concomitant crystallization of four polymorphs is reported, refcodes RUWYIR[21] and HEYHUO.[22] There is only one concomitant pentamorphic system, refcode ZZZVXQ.[23]

CONCLUSION

Four concomitant polymorphs of 2-*t*-Bu where one polymorph is chiral and other three are racemic are discussed. Crystallization of *t*-butyl fuchsone in chiral space group is rationalized. The occurrence of chiral crystallization for *t*-Bu fuchsones is ascribed to (1) inaccessible energy barrier to interconversion between chiral conformers at room temperature, (2) ready formation of C−H···O helices in the crystal structure, and (3) repulsive *t*-Bu interactions in racemic crystal structures. Crystallization of conformationally flexible fuchsone molecule in a chiral space group is noteworthy because the norm would be crystallization in centrosymmetric space groups. Moreover, the chiral crystal structure I is the most stable polymorph compared to centrosymmetric polymorphs II−IV. The transformation of form II to form III and finally to form I proceeds in a single-crystal-to-single-crystal event. Even though the detailed reasons on the role of substituent in chiral/racemic crystallization of fuchsones are yet to fully unfold, steric influence around the carbonyl group appears to be an important determinant. Controlled chiral crystallization was reproducibly achieved for 2-*t*-Bu in $P2_1$ Sohncke space group.

EXPERIMENTAL SECTION

Synthesis. The synthetic route to fuchsones from the corresponding benzophenone and 2,6-dialkyl phenol is shown in Scheme 3.[24]

2-t-Bu. 4,4′-Dimethylbenzhydrol was synthesized starting from the corresponding benzophenone (1.05 g, 5 mmol) by reaction with sodium borohydride (0.189 g, 5 mmol) in methanol. Conc. H_2SO_4 (5−6 drops) was added to a stirred solution of 2,6-ditertiarybutylphenol

dx.doi.org/10.1021/cg201652h | Cryst. Growth Des. 2012, 12, 1613−1625

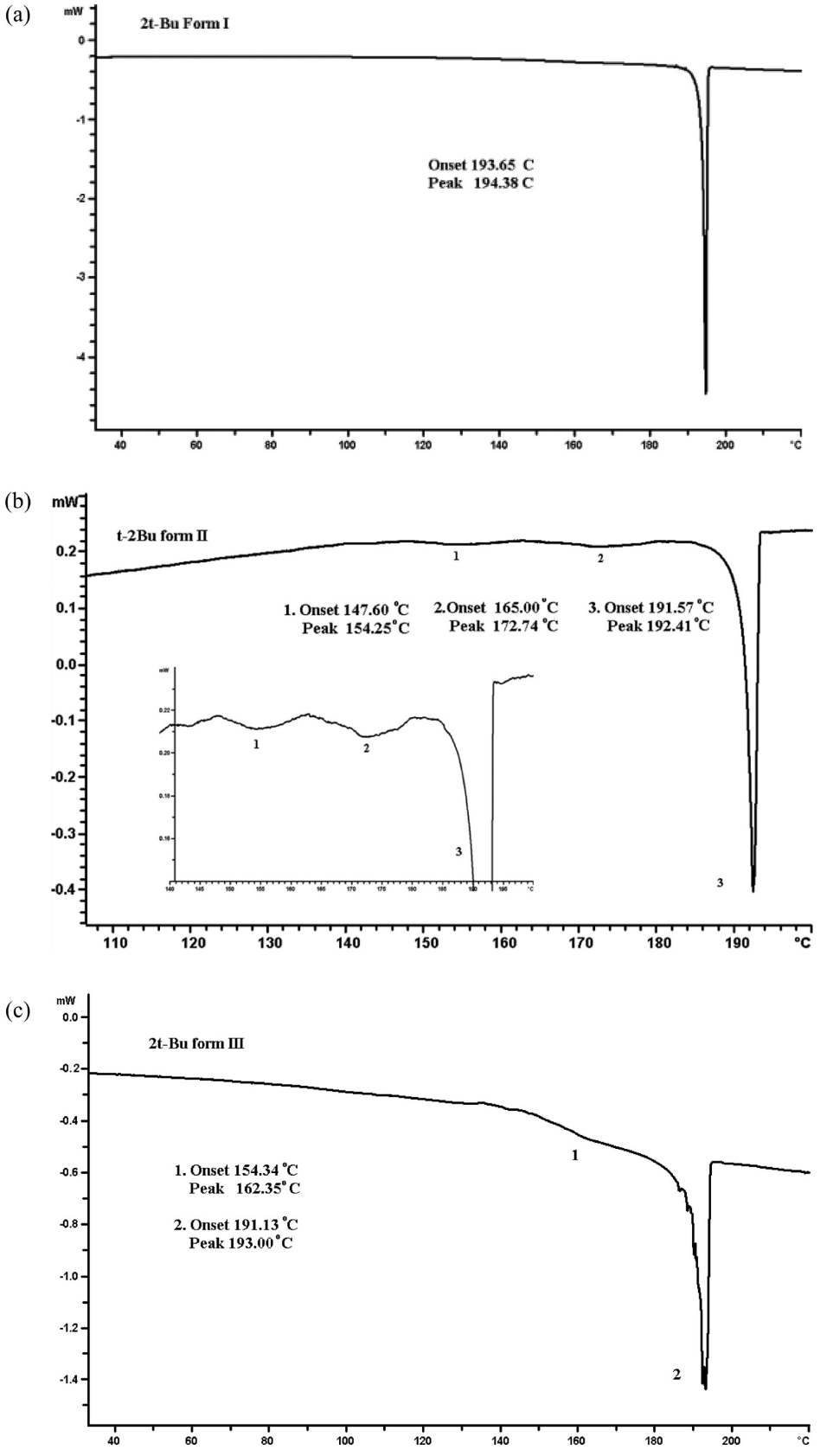

Figure 14. DSC thermograms of 2-*t*-Bu form I (a), form II (b), and form III (c). Whereas the baseline is flat for form I, there are small endo-/exotherm events noted for form II and III in the premelting stage. The details of minor thermal events are magnified in (b).

(1.03 g, 5 mmol) and 4,4′-dimethylbenzhydrol (1.06 g, 5 mmol) in acetic acid (15 mL). The precipitate obtained was filtered and dried to get 3, 5-ditertiarybutyl-4-hydroxyphenylditolylmethane. A suspension of active MnO_2 (0.870 g, 10 mmol) and 3,5-ditertiarybutyl-4-hydroxyphenylditolylmethane (1.88 g, 5 mmol) in benzene (20 mL) was stirred for 12 h and filtered. The solvent was evaporated and dried to obtain 2-*t*-Bu, which was

dx.doi.org/10.1021/cg201652h | *Cryst. Growth Des.* 2012, 12, 1613–1625

Table 5. Calculated Packing Fraction and Density (in Platon) of Four Polymorphs

form	packing fraction (%)	density (g/cm^3)
Form I	65.8	1.116(3)
Form II	62.7	1.0623(2)
Form III	62.8	1.0639(2)
Form IV	65.7	1.1171(2)

purified by column chromatography using a 2% EtOAc/hexane elution solvent.

^{1}H NMR ($CDCl_3$, ppm): 7.21 (10H, m), 2.43 (6H, s), 1.26 (18H, s).

IR (cm^{-1}): 2956, 1629, 1602, 1515.

m.p.: 187 °C.

2-i-Pr. 2-i-Pr was synthesized using the above procedure with appropriate starting materials.

^{1}H NMR ($CDCl_3$, ppm): 7.25 (4H, d, J 8), 7.15 (6H, m), 3.25 (2H, m), 2.45 (6H, s), 1.09 (12H, d, J 8).

IR (cm^{-1}): 2957, 1628, 1595.

m.p.: 178 °C.

Crystallization of Concomitant Polymorphs. A solution of 2-*t*-Bu (80 mg) in 2−3% EtOAc + *n*-hexane (20 mL) in a round bottomed flask was evaporated on a rotary evaporator at 75−80 °C. After partial/complete evaporation of the solvent, 5 mL of *n*-hexane was quickly added and poured in a conical flask to dissolve the residue. After 7−10 h crystals started appearing on the walls of the conical flask as thin plates (form II), thick plates (form III), and small needles/fibers (form IV). After complete evaporation of the solvent, block type crystals (form I) appeared on the bottom of the flask (Figure 1). This procedure was adapted from the early observation that column chromatography fraction gave the four polymorphs concomitantly. Flash evaporation in a rotary evaporator seemed to be an important step, because routine evaporation gave form I only. Details of this somewhat unusual crystallization procedure are shown in Schemes S1 and S2, Supporting Information.

Routine Crystallization of Polymorph I. Solvents such as *n*-hexane, EtOAc, benzene, toluene, mesitylene, CH_3CN, ethanol, isopropanol, *n*-propanol, *n*-butanol, acetone, etc. at ambient temperature and crystallization from $CHCl_3$, CH_2Cl_2, di-iospropyl ether, diethyl ether, and methanol at −10 °C resulted in crystalline form I.

Seeding Experiments. Seeds of forms II, III, and IV were added to obtain these polymorphs selectively in methanol and diethyl ether solvents at room temperature, but these experiments resulted in form I only.

X-ray Crystallography. Bruker SMART CCD diffractometer Mo−Kα (λ = 0.71073 Å) radiation was used to collect X-ray reflections on four polymorphs. Data reduction was performed using Bruker SAINT software.[25] Intensities for absorption were corrected using SADABS.[26] Structures were solved and refined using SHELXL-97.[27] Flack parameter was determined by collecting X-ray data on Oxford Xcalibur Gemini Eos CCD diffractometer using Cu−Kα (λ = 1.5418 Å) radiation at 100 K. Data reduction was performed using CrysAlisPro, Oxford Diffraction Ltd., Version 171.33.55. OLEX2−1.0[28] and SHELXTL 97 were used to solve and refine all data. All non-hydrogen atoms were refined anisotropically, and C−H hydrogens were fixed. X-Seed[29] was used to prepare figures and packing diagrams. Crystallographic .cif files of Mo−Kα and Cu−Kα X-ray data (CCDC Nos. 857061−857068) are available at http://www.ccdc.cam.ac.uk/data_request/cif or from the author upon request.

Thermal Analysis. DSC was performed on Mettler Toledo DSC 822e module. Samples were placed in crimped but vented aluminum pans with a sample size of 4−6 mg. DSC of form I and form III were performed at heating rate of 2 °C/min from 30 to 210 °C, whereas DSC of form II was recorded at 0.5 °C/min ramp from 100 to 200 °C. Samples were purged in a stream of dry nitrogen flowing at 150 mL/min.

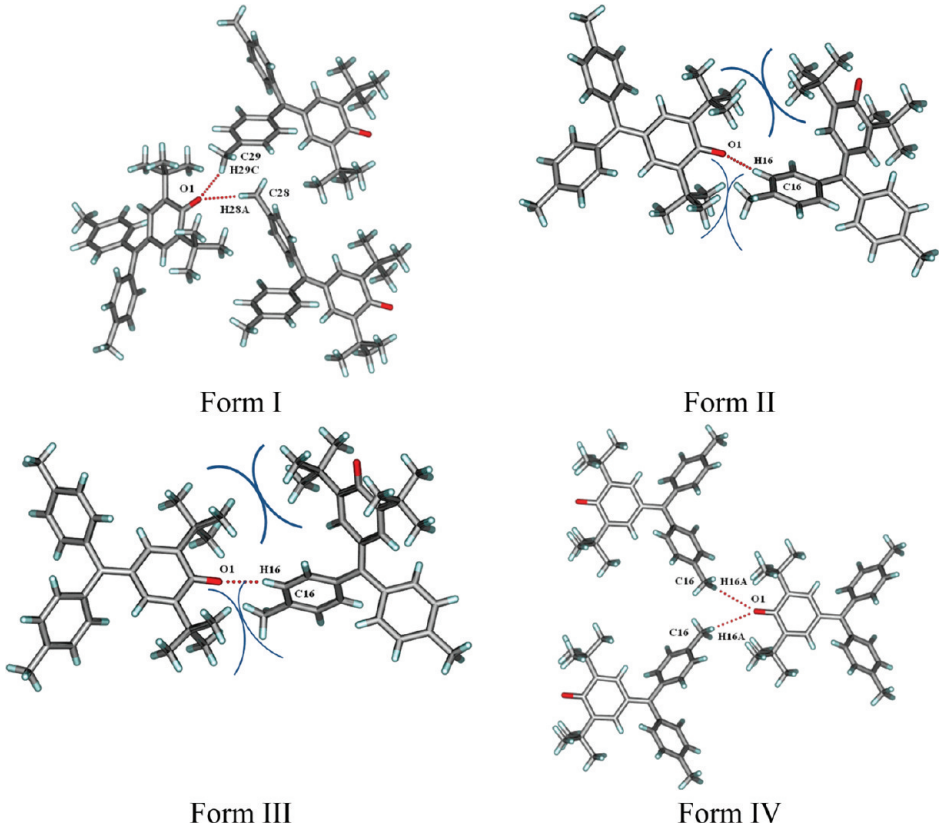

Figure 15. C−H···O hydrogen bond in form I and form IV involve *p*-methyl CH donors of tolyl ring, whereas phenyl CH ortho to the methyl group of tolyl ring is involved in forms II and form III. The bumping of alkyl groups moves the molecules farther apart in structures II and III. The C−H···O is very long in form IV (2.98 Å).

dx.doi.org/10.1021/cg201652h | *Cryst. Growth Des.* 2012, 12, 1613−1625

HSM was performed on PolythermA Hot Stage and Heiztisch microscope supplied by Wagner & Munz. A Moticam 1000 (1.3 MP) camera supported by Motic ImagePlus 2.0 ML software to record images.

CD Spectra. Solid state and solution state CD spectra were recorded on JASCO J-810 CD spectrophotometer at University of Nottingham. Solid-state CD experiments were carried out by mounting KBr pellets of form I at concentration range of 0.8−1%. Solution state CD measurements were recorded in ethanol at concentration of 10 mg/mL.

■ ASSOCIATED CONTENT

Ⓢ Supporting Information

Table S1: Crystal data on three different crystals of 2-*t*-Bu form I using Cu-Kα radiation to determine the absolute chirality; Table S2 CSD refcodes of chiral/achiral polymorph clusters containing a *t*-butyl group in the molecule; Figure S1: M helicity of 2-*t*-Bu molecule in the chiral crystal structure of polymorph I; Figure S2: Conformational change of *t*-butyl group as the Me group rotates from 130° to 150°; Figure S3: 4-*t*-Butyl-2-(2,2-dimethyl-1-methylthiopropylidene)-1,3-dithiole (CSD refcode BMTPRD); Figure S4: Phase transition (Form II to Form III to Form I). Figure S5: Phase transition (Form III to Form I). Scheme S1: Sequence of steps which afforded concomitant polymorphs of 2-*t*-Bu. Scheme S2: Standardized protocol for the reproducible crystallization of 2-*t*-Bu concomitant polymorphs in multiple batches. This material is available free of charge via the Internet at http://pubs.acs.org.

■ AUTHOR INFORMATION

Corresponding Author

*E-mail ashwini.nangia@gmail.com.

Notes

The authors declare no competing financial interest.

■ ACKNOWLEDGMENTS

This research was funded by DST (SR/S1/OC-67/2006 and SR/S2/JCB-06/2009). N.K.N. thanks the UGC for a fellowship.

■ REFERENCES

(1) (a) Jacques, J.; Collet, A.; Wilen, S. H. *Enantiomers, Racemates, and Resolutions*; Wiley: New York, 1981. (b) Sephton, M. A.; Emerson, C. R.; Zakharov, L. N.; Blakemore, P. R. *Chem. Commun.* **2010**, *46*, 2094−2096. (c) Collet, A.; Brienne, M.-J.; Jacques, J. *Chem. Rev.* **1980**, *80*, 215−230.

(2) (a) Pérez-García, L.; Amabilino, D. B. *Chem. Soc. Rev.* **2002**, *31*, 342−356. (b) Kondepudi, D. K.; Asakura, K. *Acc. Chem. Res.* **2001**, *34*, 946−954.

(3) (a) Eliel, E. L. *Stereochemistry of Carbon Compounds*; Tata McGraw-Hill: New Delhi, 1975. (b) Lunazzi, L.; Mancinelli, M.; Mazzanti, A. *J. Org. Chem.* **2008**, *73*, 5354−5359. (c) Cunningham, I. D.; Coles, S. J.; Hursthouse, M. B. *Chem. Commun.* **2000**, 61−62. (d) Tanaka, A.; Inoue, K.; Hisaki, I.; Tohnai, N.; Miyata, M.; Matsumoto, A. *Angew. Chem., Int. Ed.* **2006**, *45*, 4142−4145. (e) Sakamoto, M.; Utsumi, N.; Ando, M.; Saeki, M.; Mino, T.; Fujita, T.; Katoh, A.; Nishio, T.; Kashima, C. *Angew. Chem., Int. Ed.* **2003**, *42*, 4360−4363. (f) Zhang, J.; Chen, S.; Nieto, R. A.; Wu, T.; Feng, P.; Bu, X. *Angew. Chem., Int. Ed.* **2010**, *49*, 1267−1270.

(4) (a) Pidcock, E. *Chem. Commun.* **2005**, 3457−3459. (b) Matsuura, T.; Koshima, H. *J. Photochem. Photobiol. C: Photochem. Rev.* **2005**, *6*, 7−24.

(5) (a) Curtin, D. Y.; Paul, I. C. *Chem. Rev.* **1981**, *81*, 525−541. (b) Zyss, J.; Chemla, D. S. In *Non-linear Optical Properties of Organic Molecules and Crystals*; Zyss, J.; Chemla, D. S., Eds.; Academic Press: New York, 1987; Vols. *1 and 2*.

(6) (a) Suzuki, T.; Fukushima, T.; Yamashita, Y.; Miyashi, T. *J. Am. Chem. Soc.* **1994**, *116*, 2793−2803. (b) Sakamoto, M.; Kobaru, S.; Mino, T.; Fujita, T. *Chem. Commun.* **2004**, 1002−1003. (c) Koshima, H.; Kawanishi, H.; Nagano, M.; Yu, H.; Shiro, M.; Hosoya, T.; Uekusa, H.; Ohashi, Y. *J. Org. Chem.* **2005**, *70*, 4490−4497.

(7) (a) Guijarro, A.; Yus, M. *The Origin of Chirality in Nature*; RSC Publishing: Cambridge, 2009. (b) Avalos, M.; Babiano, R.; Cintas, P.; Jiménez, J. L.; Palacios, J. C. *Chem. Commun.* **2000**, 887−892.

(8) (a) Lewis, T. W.; Paul, I. C.; Curtin, D. Y. *Acta Crystallogr.* **1980**, *B36*, 70−77. (b) Duesler, E. N.; Lewis, T. W.; Curtin, D. Y.; Paul, I. C. *Acta Crystallogr.* **1980**, *B36*, 166−168.

(9) (a) Chandran, S. K.; Nath, N. K.; Roy, S.; Nangia, A. *Cryst. Growth Des.* **2008**, *8*, 140−154. (b) Nath, N. K.: Nangia, A., unpublished results.

(10) Bernstein, J.; Davey, R. J.; Henck, J.-O. *Angew. Chem., Int. Ed.* **1999**, *38*, 3440−3461.

(11) (a) Kalsi, P. S. *Streochemistry Conformation and Mechanism*; New Age International (P) Limited Publishers: New Delhi, 2008; p 149. (b) March, J. *Advanced Organic Chemistry: Reactions, Mechanisms and Structure*, 4th ed.; Wiley Interscience: New York, 1992; pp 103−104. (c) Wolf, C. *Dynamic Stereochemistry of Chiral Compounds: Principles and Applications*; The Royal Society of Chemistry: Cambridge, 2008; pp 53−54.

(12) Nangia, A. *Acc. Chem. Res.* **2008**, *41*, 595−604.

(13) Flack, D. *Acta Crystallogr.* **1983**, *A39*, 876−881.

(14) (a) Pescitelli, G.; Pietro, S. D.; Cardellicchio, C.; Capozzi, M. A. M.; Bari, L. D. *J. Org. Chem.* **2010**, *75*, 1143−1154. (b) Minguet, M.; Amabilino, D. B.; Wurst, K.; Veciana, J. *J. Chem. Soc., Perkin Trans.* **2001**, *2*, 670−676. (c) Hao, H.-Q.; Liu, W.-T.; Tan, W.; Lin, Z.-J.; Tong, M. -L. *CrystEngComm* **2009**, *11*, 967−971. (d) Sun, Q.; Bai, Y.; He, G.; Duan, C.; Lin, Z.; Meng, Q. *Chem. Commun.* **2006**, 2777−2779.

(15) (a) Lennartson, A.; Wiklund, T.; Håkansson, M. *CrystEngComm* **2007**, *9*, 856−859. (b) Vestergren, M.; Johansson, A.; Lennartson, A.; Håkansson, M. *Mendeleev Commun.* **2004**, 258−260. (c) Lennartson, A.; Vestergren, M.; Håkansson, M. *Chem.—Eur. J.* **2005**, *11*, 1757−1762.

(16) Cambridge Crystallographic Data Center, www.ccdc.cam.ac.uk.

(17) (a) Hu, C.; Englert, U. *Angew. Chem., Int. Ed.* **2005**, *44*, 2281−2283. (b) Avarvari, N.; Faulques, E.; Fourmigué, M. *Inorg. Chem.* **2001**, *40*, 2570−2577. (c) Supriya, S.; Das, S. K. *J. Am. Chem. Soc.* **2007**, *129*, 3464−3465. (d) Zhang, Y.-J.; Liu, T.; Kanegawa, S.; Sato, O. *J. Am. Chem. Soc.* **2009**, *131*, 7942−7943. (e) Vittal, J. J. *Coord. Chem. Rev.* **2007**, *251*, 1781−1795. (f) Kaftory, M.; Botoshansky, M.; Kapon, M.; Shteiman, V. *Acta Crystallogr.* **2001**, *B57*, 791−799. (g) Takahashi, H.; Ito, Y. *CrystEngComm* **2010**, *12*, 1628−1634. (h) Das, D.; Engel, E.; Barbour, L. J. *Chem. Commun.* **2010**, *46*, 1676−1678. (i) Görbitz, C. H. *J. Phys. Chem.* **2011**, *B115*, 2447−2453. (j) Atwood, J. L.; Barbour, L. J.; Jerga, A.; Schottel, B. L. *Science* **2002**, *298*, 1000−1002.

(18) Ostwald, W. F. *Z. Phys. Chem.* **1897**, *22*, 289−330.

(19) Wallach, O. *Liebigs Ann. Chem.* **1895**, *286*, 90−143.

(20) Brock, C. P.; Schweizer, W. B.; Dunitz, J. D. *J. Am. Chem. Soc.* **1991**, *113*, 9811−9820.

(21) Morimoto, M.; Kobatake, S.; Irie, M. *Chem.—Eur. J.* **2003**, *9*, 621−627.

(22) Kumar, V. S. S.; Addlagatta, A.; Nangia, A.; Robinson, W. T.; Broder, C. K.; Mondal, R.; Evans, I. R.; Howard, J. A. K.; Allen, F. H. *Angew. Chem., Int. Ed.* **2002**, *41*, 3848−3851.

(23) Parrish, D. A.; Deschamps, J. R.; Gilardi, R. D.; Butcher, R. J. *Cryst. Growth Des.* **2008**, *8*, 57−62.

(24) Becker, H.-D. *J. Org. Chem.* **1967**, *32*, 2131−2136.

(25) *SAINT-Plus*, version 6.45; Bruker AXS Inc.: Madison, WI, 2003.

(26) Sheldrick, G. M. *SADABS, Program for Empirical Absorption Correction of Area Detector Data*; University of Göttingen: Germany, 1997.

(27) (a) *SMART (Version 5.625) and SHELX-TL (Version 6.12)*; Bruker AXS Inc.: Madison, WI, 2000; (b) Sheldrick, G. M. *SHELXS-97 and SHELXL-97*; University of Göttingen, Germany, 1997.
(28) Dolomanov, O. V.; Blake, A. J.; Champness, N. R.; Schröder, M. *J. Appl. Crystallogr.* **2003**, *36*, 1283−1284.
(29) Barbour, L. J. *X-Seed, Graphical Interface to SHELX-97 and POV-Ray*, University of Missouri-Columbia, Columbia, MO, 1999.